AAS 98-340

TEST OF A FLEXIBLE SPACECRAFT DYNAMICS SIMULATOR

Donald Dichmann* and Joseph Sedlak†

There are a number of approaches one can take to modeling the dynamics of a flexible body. While one can attempt to capture the full dynamical behavior subject to disturbances from actuators and environmental torques, such a detailed description often is unnecessary. Simplification is possible either by limiting the amplitude of motion to permit linearization of the dynamics equations or by restricting the types of allowed motion. In this work, we study the nonlinear dynamics of bending deformations of wire booms on spinning spacecraft. The theory allows for large amplitude excursions from equilibrium while enforcing constraints on the dynamics to prohibit those modes that are physically less relevant or are expected to damp out fast. These constraints explicitly remove the acoustic modes (i.e., longitudinal sound waves and shear waves) while allowing for arbitrary bending and twisting motions which typically are of lower frequency.

As a test case, a spin axis reorientation maneuver by the Polar Plasma Laboratory (POLAR) spacecraft has been simulated. POLAR was chosen as a representative spacecraft because it has flexible wire antennas that extend to a length of 65 meters. Bending deformations in these antennas could be quite large and have a significant effect on the attitude dynamics of the spacecraft body. Summary results from the simulation are presented along with a comparison with POLAR flight data.

INTRODUCTION

This work describes the design and application of a flexible spacecraft dynamics simulator, named Cartwheel, to model a spin axis reorientation maneuver by the Polar Plasma Laboratory (POLAR) spacecraft. It presents a summary of the simulation results and a comparison with flight data. Overviews of the theory and the software are also given.

The general purpose of this research was to study the applicability of a particular flexible dynamics method to spacecraft attitude dynamics. As described below, the Cartwheel simulator captures the most important parts of the nonlinear dynamics but leaves out a number of smaller effects. As a prototype analysis tool, Cartwheel has been used for basic theoretical tests but is not intended for operations support.

* The Aerospace Corporation, 2350 El Segundo Blvd., El Segundo, CA, USA 90245.

† Computer Sciences Corporation (CSC), 10110 Aerospace Rd., Seabrook, MD, USA 20706.

We chose POLAR as a representative spacecraft because it has flexible wire antennas that extend up to 65 m in length, so the wire antennas contribute a large fraction of the total moment of inertia. Due to the great length of these thin wire booms, bending deformations can have a significant effect on the attitude dynamics of the hub of the spacecraft body. Flexure of the antennas can cause large changes in the total moment of inertia, which, in turn, can affect the spacecraft rotation rate. The motions of the antennas couple through the rigid hub. In addition, the antennas have some intrinsic stiffness, that is, a tendency to spring back to their default orientation (normally straight). The resulting highly nonlinear dynamics leads to complex perturbations to the attitude.

The POLAR spacecraft periodically executes a 180 degree spin reorientation maneuver to prevent the Sun from coming into view of certain instruments. We anticipated that this type of maneuver would induce vibration in the wire booms that could measurably influence the attitude dynamics of the hub. This paper describes the application of the Cartwheel simulator to such a maneuver.

The next sections contain overviews of the dynamics theory and the Cartwheel software. This is followed by a description of the POLAR spacecraft, orbit, attitude, and the spin axis reorientation maneuver. Finally, a summary of the simulation results and comparison with POLAR flight data is given.

THEORY

The flexible spacecraft dynamics simulation program, Cartwheel, was designed to model the nonlinear dynamics of large bending deformations of wire booms on spacecraft. In these simulations, we enforce constraints on the dynamics to prohibit the generally lower amplitude, higher frequency acoustic modes (i.e., longitudinal sound waves and shear waves) but to allow the larger, lower frequency bending and twisting motions. While it is possible to model the full dynamical problem, this is made difficult by the presence of both very slow and very fast characteristic appendage motions. Describing all the characteristic frequencies accurately leads to difficulties and inefficiencies when integrating the governing equations. Dynamical systems with this problem are called *stiff*. There are two broad kinds of simplifications that make solution of the governing equations more tractable. One can assume the deviations of the appendages from their equilibrium positions are of low amplitude and then discard all terms in the equations that are of second or higher order in this amplitude. The resulting linear system of equations can be analyzed in terms of its normal modes of vibration. Alternatively, one can disallow types of motion that are physically less important for the system under consideration. The approach taken in this work is to discard the generally high frequency motions associated with stretching and shearing of the appendages (acoustic modes) while keeping the full nonlinear description of the rest of the motion (flexing and twisting).

Constraining the dynamics to disallow acoustic modes makes numerical solutions easier to obtain without appreciably limiting their validity. The only motions of interest here are those that affect the spacecraft attitude; these are likely to be combinations of simple oscillations and possibly "whiplash" motions of the booms. These motions are not likely to excite or couple strongly to the acoustic modes. In addition, acoustic modes are likely to damp out fast in the multi-stranded boom material. Eliminating these modes from the start is very nearly the same as describing the full dynamics of a system with highly damped acoustic modes.

The method chosen for enforcing the dynamical constraints is called the *impetus-striction* method (Ref. 1). The method has proven valuable in theoretical analyses of stability conditions (Ref. 2) as well as in numerical simulations to rod dynamics (Ref. 3). The key features of the impetus-striction method are as follows:

- The method applies to systems having a Lagrangian formulation subject to holonomic constraints. It transforms constrained Lagrangian dynamics into an unconstrained Hamiltonian formulation where constraints appear as constants of the motion.
- Each constraint equation is replaced by its time-derivative; the Lagrange multipliers associated with these time-differentiated constraints are called the *strictions* and have dimensions of momentum.
- One derives the conjugate variables to be used in the Hamiltonian formulation from the constrained Lagrangian (the classical Lagrangian plus constraint terms). Thus, the conjugate variables are not quite the same as the usual momentum variables that arise from the classical Lagrangian alone; these new variables are the *impetuses.*
  - Roughly speaking, the striction describes that part of the momentum arising from the constraint forces, and the impetus describes that part due to the remaining forces. Note that if there are no external forces, it is still the total momentum that is conserved, not the impetus.
- One constructs a "pre-Hamiltonian" from the constrained Lagrangian; this differs from the usual Hamiltonian only in that it still depends on the as yet undetermined strictions.
- The Hamiltonian is obtained by minimizing the pre-Hamiltonian with respect to the strictions for fixed values of the state variables. This minimization determines the strictions and can usually be reduced to the solution of a system of linear algebraic equations.
- The resulting unconstrained Hamiltonian system is integrated in time, solving for the strictions at each time step.

OVERVIEW OF CARTWHEEL

The physical model of the boom dynamics yields a system of nonlinear partial differential equations in which the independent variables are time and arc length along each boom, both of which must be discretized for the numerical implementation.

For the discretization in arc length (often called the semi-discretization), we model each boom as a sequence of N_n elastically connected rigid segments. As implemented, the integration errors are of order h^2 as the segment length, h, goes to zero, and the errors vanish for any segment length when the spacecraft rotates uniformly with zero deflection in the wires.

There is a position and orientation associated with each boom segment. Orientations are represented by quaternions, so there are seven configuration variables for each segment, along with their conjugates (the impetuses). Note that the quaternion normalizations are not imposed by brute force but are maintained by the integration method. There are N_a antennas (N_n can be different for each antenna). There also is a position and orientation for the spacecraft hub and a position for the center of mass of the entire system.

For each time step, the strictions are calculated as the solution of a linear system of equations; the number of strictions is $3N_nN_a$ representing the stretch and shear constraints for each segment, plus $3N_a$ to constrain the position of the antenna attachments to the hub, plus 3 more to separate relative position coordinates from the system center of mass. (The striction equations decouple into N_a banded, linear systems, each with $3N_n$ unknowns, together with the solution of one system with $3N_a$ unknowns, and one with 3 unknowns for the center of mass.)

For the discretization in time, the Hamiltonian system, consisting of $(14N_nN_a + 20)$ first-order ordinary differential equations for the coordinates and conjugate impetuses, is stepped forward using a midpoint method. That is, if z^k is the state at time t_k and $F(z)$ is its time derivative, then

$$z^{k+1} = z^k + \Delta t\, F\left(\frac{z^{k+1} + z^k}{2}\right) \tag{1}$$

This is an implicit integration scheme wherein the time derivative evaluation requires knowledge of the new state. Implicit methods are numerically more stable than explicit methods but require solution of a possibly nonlinear system of equations for z^{k+1} at each time step. Equation (1) is solved by a fixed-point iteration method but a Newton method could also be used.

The integrator was chosen not only for its inherent stability but because it is one of the simplest of the symplectic integration methods. One consequence of this is that it preserves quadratic invariants (see, for example, Ref. 4). This means that any theoretical constant of the motion that is quadratic in the state variables will not be subject to any numerical error beyond machine roundoff. In practice, the error level is determined by the tolerance allowed when iterating for a solution to Eq. (1).

Some examples of quadratic invariants are the quaternion norms and the amount of stretch and shear between segments of the appendages. Other invariants may depend on the boundary conditions of a particular example. For this problem, total linear momentum and total angular momentum are quadratic invariants. On the other hand, although the total energy is a conserved quantity (there is no damping in the model), the Hamiltonian is not quadratic in the state variables. Consequently, the code is not expected to conserve the energy as well as the quadratic invariants.

Note that this formalism enforces the constraints by solving for and imposing the requisite forces, and the resulting *augmented* Hamiltonian system is unconstrained. Thus, while the stretch and shear are constrained to vanish, they are not set to zero *ad hoc*. They are free to take on any value but remain small only because of the imposed forces (the strictions). The point here is that the finite step size in the time-integration scheme could conceivably cause growing errors in the constraints. The use of a symplectic integrator guarantees that this will not happen.

The first test of the code was to examine the invariants. The errors in the quadratic invariants should remain small (close to the tolerance of the solution of Eq. (1)), and the error in the total energy should grow with a slope proportional to the time step squared. This has been demonstrated remarkably well for both single rod and closed ring simulations (Ref. 3). (Interest in these early rod and ring tests goes beyond just verifying the impetus-striction method. They are well suited for modeling some aspects of biomolecules such as bacterial DNA (Ref. 5).)

Later tests verified that the invariants are properly conserved also for the full spacecraft model (multiple booms coupled through a rigid hub) and that accurate results are obtained for small perturbations with the booms discretized into relatively few segments.

THE POLAR SPACECRAFT

The mission of the POLAR spacecraft is to observe the electromagnetic field of the Earth's polar regions. The hub of the spacecraft is about 1.58 m in radius. The mass is roughly 1000 kg. Nominally, the spacecraft spins at a rate of 10 revolutions per minute (rpm) with the spin axis oriented near the orbit normal vector. Spin axis direction is determined using a Sun sensor and an Earth sensor. The spacecraft has two axial booms extending along the positive and negative spin axes. The axial booms are effectively rigid and are rigidly attached to the spacecraft hub. The spacecraft also has two radial booms, holding magnetometers, that are effectively rigid and rigidly attached to the spacecraft hub.

The spacecraft has four flexible wire booms extending radially from the hub and arranged symmetrically. Each wire boom can be deployed to a maximum length of 65 m. Each wire has a radius of 1 mm. The wire booms serve as antennas to observe the ambient electromagnetic field and also to help stabilize the spacecraft rotation. During the phase of the mission treated in this study, one pair of wire booms was deployed to 50 m while the other was deployed to 65 m.

The POLAR spacecraft orbits the Earth in a near polar, elliptical orbit (roughly 2×9 Earth radii). The pre-maneuver orbit had semimajor axis equal to 34251 km, the eccentricity was 0.662, the inclination was 86.01 deg, and the right ascension of the ascending node was 26.809 deg. The orbital period is approximately 12 hours.

During most of the mission, the spacecraft spin axis is maintained along the positive or negative orbit normal. As the Sun-orbit plane geometry changes, it is necessary about every 6 months to reorient the spin axis for solar thermal constraints and to keep the Sun out of the field of view of sensitive instruments. At those times, the spin axis is reoriented by 180 deg from positive to negative orbit normal, or vice versa. This is done while keeping the Sun vector nearly perpendicular to the spin axis. Due to current thruster limitations, this maneuver is performed in two separate 90 degree slews, each lasting roughly 3.5 hours.

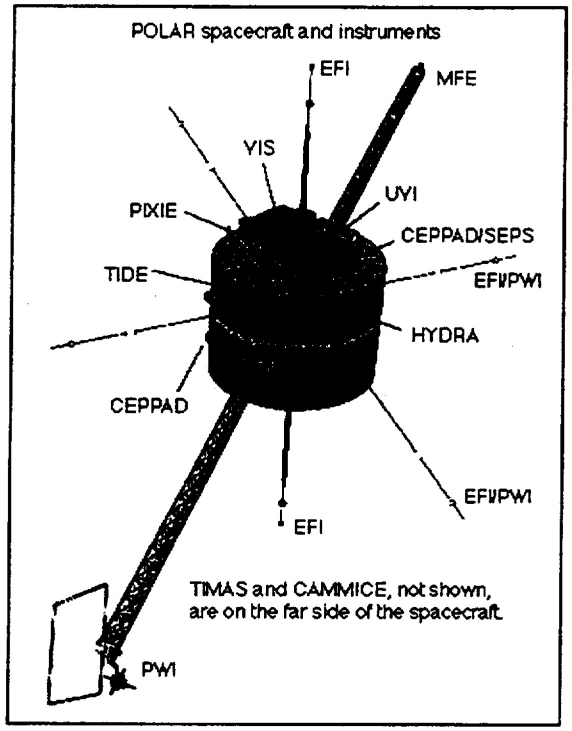

Figure 1. The POLAR spacecraft and instruments.

This study discusses one such maneuver that was performed on April 16-17, 1996. We anticipated that the maneuver, although performed slowly, would induce small vibrations in the flexible wire booms. There are no instruments onboard the spacecraft to measure directly the deformations of the booms. However, due to their length during this phase of the mission, the booms contribute about 50% of the total moment of inertia about the spacecraft's spin axis. It was therefore expected that if there were any flexure of the booms, this would have a measurable effect on the attitude of the spacecraft hub.

SIMULATION RESULTS

In this section, we describe the results of numerical simulations of the POLAR spin reorientation maneuver and compare results from flexible and rigid body models. Our simulations focused upon the effects of boom flexibility on the attitude dynamics of the spacecraft hub. Because of their length, the booms could exhibit large bending motions under the appropriate circumstances. However, because the spacecraft spins at 10 rpm, each boom experiences a stiffening centrifugal force that tends to inhibit deformations. In addition, the rate of the spin reorientation maneuver is small (90 degrees in 3.5 hours), so the perturbing forces and torques acting on the booms are small. For these reasons, only small deformations of the wire booms were found.

To display the deformations, the position of the end of each segment is represented in a rotating body coordinate system attached to the spacecraft hub. If a boom continued to point radially outward from the hub, as it does during a steady spin, then the boom would exhibit no motion in this body frame. During the simulation of the spin reorientation maneuver, each boom oscillated primarily out of the spin plane and parallel to the hub's spin axis, designated as the z-axis. This motion is shown in Figure 2, where the tip's displacement is plotted as a function of time each 0.5 second. The spacecraft rotates 200 times during the 20 minute period shown. In Figure 2, the displacement is displayed as a fraction of the boom length, which is 50 meters. The amplitude of the oscillation is about 0.014 of the total length, or about 0.7 m.

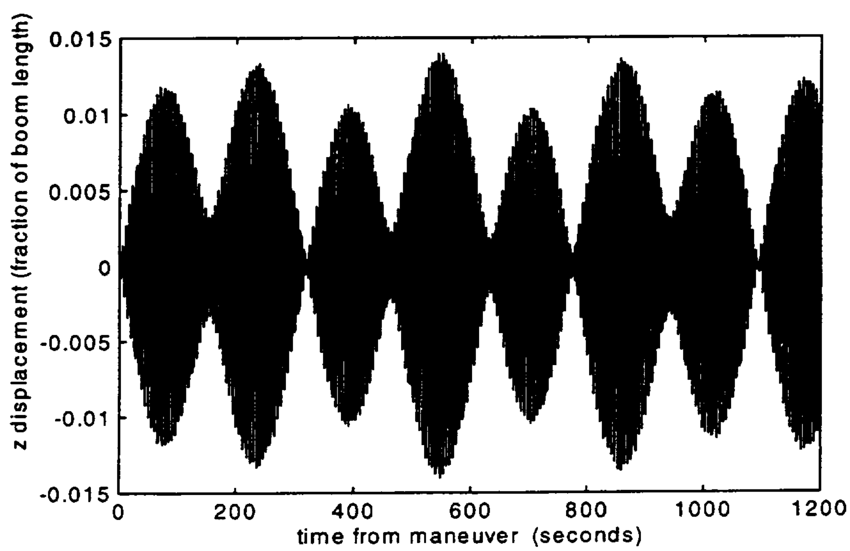

Figure 2. Out-of-plane displacement of boom tip for model with two unequal length pairs of wire booms (peak amplitude corresponds to 0.7 m).

The complex motion in Figure 2 can be approximated well by a superposition of three distinct oscillations:

$$z(t) = \sum_{j=1}^{3} A_j \cos(2\pi t / T_j) + B_j \sin(2\pi t / T_j) \tag{2}$$

where the periods are T_1 = 6.0 sec, T_2 = 5.778 sec, and T_3 = 5.872 sec. The amplitudes are $A_1 = -5.25\times10^{-3}$, $B_1 = 2.8\times10^{-6}$, $A_2 = 6.91\times10^{-3}$, $B_2 = -3.6\times10^{-5}$, $A_3 = -1.85\times10^{-3}$, and $B_3 = 1.3\times10^{-6}$.

The oscillation with 6 sec period is associated with the spin rate of the spacecraft. The other two frequencies appear to be associated with driven oscillations of the two pairs of booms of length 50 m and 65 m, respectively. To test this, we ran a simulation with equal length booms and all other parameters the same. The resulting motion of the tip of each boom was less complex and decomposed into the sum of oscillations with only two distinct periods of 6.00 sec and 5.79 sec as shown in Figure 3.

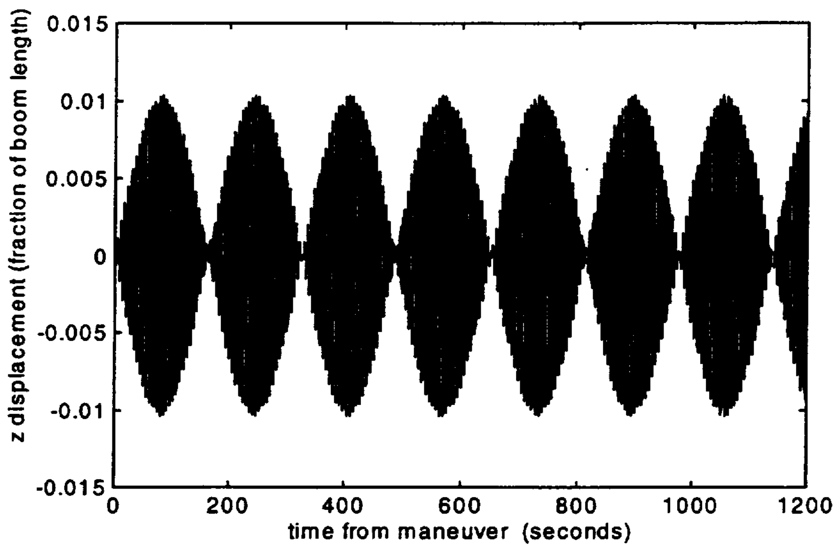

Figure 3. Out-of-plane displacement of boom tip for model with four equal length booms (peak amplitude corresponds to 0.5 m).

Although the motion of the tip of each boom is fairly complex, each boom moves nearly as a rigid rod. To demonstrate this, Figure 4 shows the maximum deviation of a boom from the straight line between its base and its tip. Thus, the oscillations shown in Figure 2 are subtracted out, leaving only the deviation caused by any curvature of the

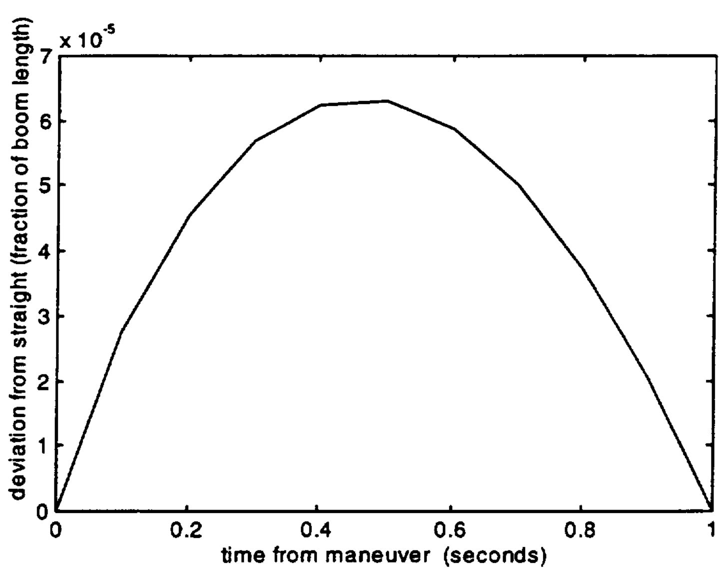

Figure 4. Maximum deviation of boom from straight line (peak amplitude corresponds to 3 mm).

boom. Again, the displacement is measured as a fraction of the boom length. The maximum displacement from the straight configuration is seen to be only about 6×10^{-5} times the 50 m length, or 3 mm.

Because each boom behaves essentially as a rigid body, the most significant flexibility effects can be captured by representing each boom as a rigid rod attached to the hub by a flexible hinge. Simulations with various, reasonable amounts of spring force in the hinge at the base show that even this elasticity has only a small effect. Thus, one can set the deformation restoring force to zero at the base.

In this simulation, the initial conditions were taken from the April 1996 reorientation maneuver. The spin axis was initially pointing toward right ascension 116.3 deg and declination -7.7 deg. The final attitude following the first 90 deg maneuver segment was estimated to be right ascension 27.2 deg and declination -80.0 deg (Ref. 6). Figure 5 shows the right ascension and declination of the hub for the simulated maneuver. For comparison, the simulation for a totally rigid spacecraft with the same mass properties is also shown. (Note that the initial attitude differs somewhat from values given in Ref. 6. This small offset is caused by a different choice of sensor biases solved for together with the attitude and does not affect the analysis.)

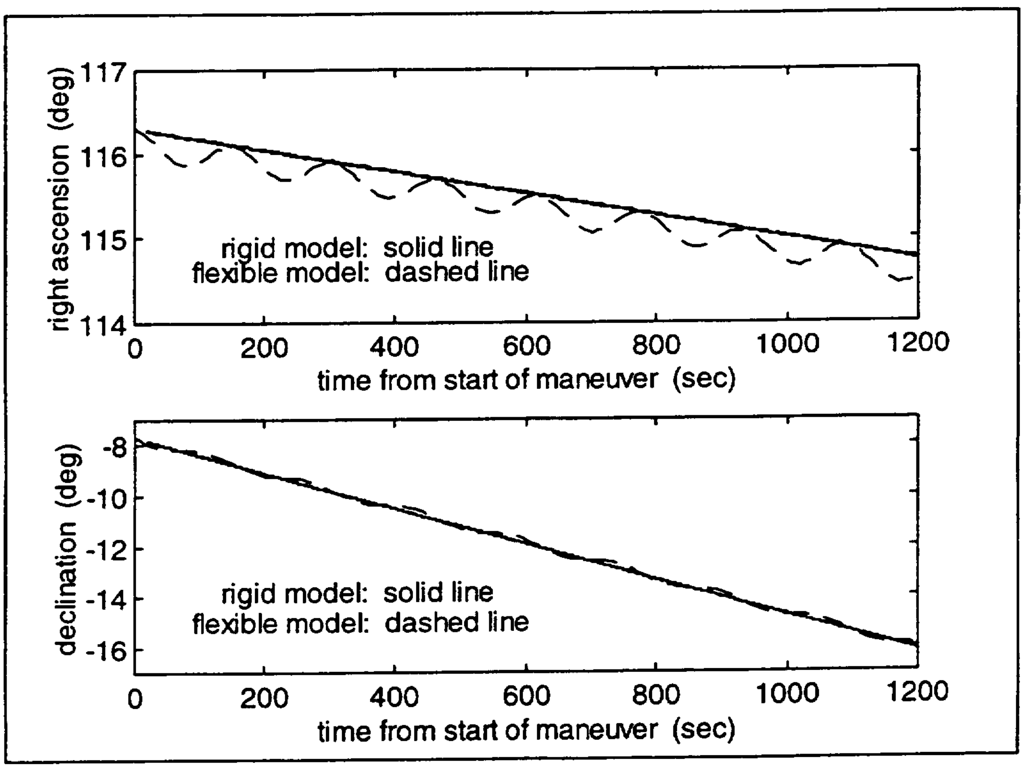

Figure 5. Rigid body and flexible model simulations showing right ascension and declination of spin axis for the first 1200 seconds of spin reorientation maneuver.

Comparison of the two simulations (flexible and rigid body) allows the effects of flexibility to be seen clearly. The flexible body simulation shows sinusoidal oscillations absent from the rigid body simulation. The period of the oscillation is about 2.6 minutes. The maximum difference in right ascension between rigid and flexible model is about 0.3 degrees. The maximum difference in declination is about 0.15 degrees. (There also are higher frequency oscillations in the rigid body attitude due to nutation that are too low in amplitude to show clearly on these plots.)

It should be noted that the flexible dynamics simulator neglects several perturbing forces that could influence the spacecraft motion. It is expected that most of these disturbances are negligible for the case under consideration. For example, gravity-gradient torques are not included. The spacecraft is near apogee during the maneuver, so the large distance from the Earth (9 Earth radii) greatly reduces the influence of gravity-gradient torque.

Internal dissipation within the wire booms could have a more significant effect on the dynamics. In particular, internal dissipation tends to damp out oscillations in the wires. Thus the current model would not yield physically correct results over long periods of time, but should be accurate for times shorter than the decay time. This is observed to be on the order of tens of minutes (see results below). An accurate model of internal dissipation could be difficult, due to the complex composite structure of the wire, and would require a more detailed knowledge of the material parameters.

The driving torque was modeled as continuous and constant. In reality, thrusters are used to supply the torque. They are fired in pulses, timed with the spin period, to perform the maneuver. The periodic pulsing of the control torque is expected to excite higher frequency vibrations of the wires that are not excited in the model.

Thermal effects are known to influence the dynamics on other spacecraft. However, these tend to be small and brief disturbances. Furthermore, for the orbital geometry during this reorientation maneuver, the POLAR spacecraft does not enter the Earth's shadow so the wire temperature is not expected to vary significantly.

Some other effects one might consider are perturbations due to atmospheric drag and fuel slosh. However, the spacecraft is at a sufficiently high altitude that torques from atmospheric drag are negligible, and fuel slosh is not a factor because the maneuver is performed sufficiently slowly compared to the spin rate.

COMPARISON OF SIMULATION WITH FLIGHT DATA

To estimate the true attitude of the POLAR spacecraft during the maneuver, the spacecraft telemetry was processed using an Attitude Ground Support System (Ref. 7) designed for spinning spacecraft. Attitude estimation was based upon Earth horizon sensor and spinning Sun sensor readings. The Earth and Sun angle measurements later were reprocessed using MATLAB where it was possible to insert sensor biases overlooked in the initial processing. In particular, this reprocessing corrected timing errors and rejected spurious solutions.

Knowing the Sun and Earth reference vectors, the measured Earth midscan angle yields the angle from the spin axis to the nadir vector with twofold ambiguity. (As the spacecraft spins, the Earth is measured as a time offset from the Sun pulse. This is converted into an angle using the spin period determined from the time between Sun pulses.) The spin axis then is found at the intersection of the two cones defined by the nadir and Sun angles (another twofold ambiguity). Knowing the path of the planned maneuver made it simple to select the correct solution. (The initial spin direction is unambiguously estimated from a large batch of data obtained before the slew.) Reference 8 gives details on methods for spacecraft attitude determination.

Figure 6 shows the estimated spin axis right ascension and declination angles for POLAR during the interval 03:16:46 GMT to 03:40:06 GMT, on April 16, 1996. The spin reorientation maneuver begins at time 03:20:06 GMT. The results of the flexible dynamics simulation from Figure 5 are also overlaid on Figure 6.

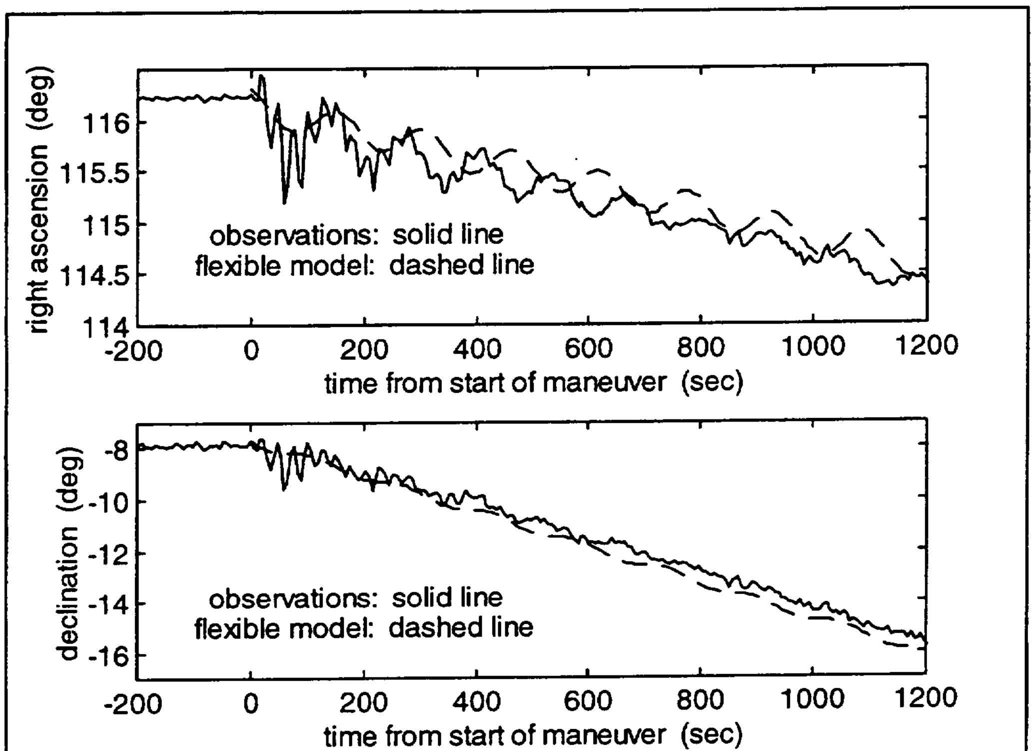

Figure 6. Observed and simulated spin axis attitude for the first 1200 seconds of spin reorientation maneuver (observations are from POLAR spacecraft maneuver on April 16, 1996).

As the maneuver progresses, the Earth horizon sensor scans across the Earth along various chords. The scan cone moves off the Earth at 03:42:58 GMT (time = 1372 sec, off scale on Figure 6). After that time, only Sun data is available and there is insufficient information to compute an attitude until the Earth again comes into view near the end of the maneuver. The estimated attitude also is less reliable due to larger Earth sensor uncertainty during the minutes immediately before the Earth horizon signal is lost. Thus, although this 90 deg segment of the maneuver takes 3.5 hrs, the attitude is observable only for the first 23 min while both the Sun and Earth are detectable, and the final 3 min are discarded.

As seen in Figure 6, the flexible body model exhibits oscillations that are qualitatively similar to the oscillations in the observed flight data. These slow oscillations are not present in the rigid body model in Figure 5. The flexible model oscillations match up exactly with the envelope of the boom tip displacements shown in Figure 2 and probably correspond to a beat frequency between two out-of-plane modes.

The quantitative features of the slow oscillations depend primarily on the material parameters of the wire booms, in particular the mass density and the bending stiffnesses. The periods are approximately 2.6 min for the flexible simulation and 2.2 min for the observed attitude. This 15% difference might be attributed to uncertainties in the material parameters available to us.

There also is fairly good agreement between the simulated and observed amplitudes, however the observed oscillation decays with time while the amplitude of the simulation does not. This reflects the absence of dissipative terms in the dynamics model. As expected, there also are higher frequency oscillations (dominated by a mode with a 30 sec period) that are not found in the simulation results. The simulation would likely have shown a much richer spectrum if the model had included more realistic pulsed thrusters rather than a continuous control torque.

CONCLUSIONS

In this study we have examined the attitude of the POLAR spacecraft during a reorientation maneuver of the spin axis. The attitude computed using flight telemetry was compared with simulated data obtained by modeling the spacecraft as a rigid hub with four flexible wire booms. A comparison with a totally rigid body model also was given. The flexible model simulation captures the most important qualitative features of the flight data and is in reasonable quantitative agreement, as well.

The Cartwheel simulator employs an implicit midpoint time-stepping scheme to perform the numerical time integration and to preserve the dynamics constraints to a high accuracy. If high numerical accuracy is not maintained, the simulation will diverge after only a few minutes of simulated dynamics. The price for high accuracy is relatively slow computational speed. For example, with each boom represented as a single rigid rod, twenty minutes of simulated data required about ten minutes of CPU time on a DEC Alpha workstation. When each boom was subdivided into five-meter segments, yielding 46 segments in all, then twenty minutes of simulated data required about ten hours of CPU time.

A number of features could be added to Cartwheel to improve its accuracy. The most important additional feature would be a more complete actuator model, particularly pulsed thrusters. Following this, one could improve the modeled material properties of the wire booms, including dissipation and more accurate mass and stiffness parameter values. Environmental perturbations could contribute small corrections, and sophisticated control laws would allow testing a wider variety of scenarios. These improvements could be implemented without making major changes to the underlying flexible dynamics model. With these additions, Cartwheel would be useful as an analysis tool to study the nonlinear dynamics of extended systems such as long-boom spinners or tethered satellites. Its strength would be most apparent for applications to systems under contingency conditions where the deformations are too extreme to be described using linearized or modal dynamics.

ACKNOWLEDGMENTS

This work was performed under a cooperative agreement among the National Science Foundation (Industrial Postdoctoral Fellowship award number 9505450), the National Aeronautics and Space Administration/Goddard Space Flight Center (contracts GS-35F-4381G and NAS 5-31000), Computer Sciences Corporation, and the University of Maryland Institute for Physical Science and Technology. Additional support came from the Air Force Office of Scientific Research. The authors would particularly like to thank Professor John Maddocks, currently at the Swiss Federal Institute of Technology, who provided guidance for much of the theoretical work that preceded the simulator development.

REFERENCES

1. D. J. Dichmann, *Hamiltonian Dynamics of a Spatial Elastica and the Stability of Solitary Waves,* Ph. D. thesis, University of Maryland, 1994.
2. D. J. Dichmann, J. H. Maddocks, and R. L. Pego, "Hamiltonian Dynamics of an Elastica and the Stability of Solitary Waves," *Arch. of Rational Mech.*, to appear.
3. D. J. Dichmann and J. H. Maddocks, "An Impetus-Striction Simulation of the Dynamics of an Elastica," *J. Nonlinear Sci.*, Vol. 6, 1996, pp. 271-292.
4. J. M. Sanz-Serna and M. P. Calvo, *Numerical Hamiltonian Problems*, Chapman and Hall, 1994.
5. M. Tabor and I. Klapper, "Dynamics of Twist and Writhe and the Modeling of Bacterial Fibers," in *Mathematical Approaches to Biomolecular Structure and Its Applications,* **82**, Springer, New York, 1996, pp. 139-160.
6. J. Dibble and S. Good, "Interplanetary Physics Laboratory (WIND) and Polar Plasma Laboratory (POLAR) Postlaunch Report," Goddard Space Flight Center, Flight Dynamics Division, 553-FDD-96/006R0UD0, July 1994.
7. A. Calder, "Multimission Spin-Axis Stabilized Spacecraft (MSASS) Flight Dynamics Support System User's Guide, Update 1," Goddard Space Flight Center, Flight Dynamics Division, 552-FDD-91/019R0UD1, March 1993.
8. J. S. Wertz, ed., *Spacecraft Attitude Determination and Control*, D. Reidel Publishing Co., Dordrecht, The Netherlands, 1978.